



Augmenting System Inertia Through Fast Acting Reserve – A power System Case Study with High Penetration of Wind Power

Rezkalla, Michel Maher Naguib; Marinelli, Mattia

Published in:
Proceedings of 54th International Universities Power Engineering Conference

Link to article, DOI:
[10.1109/UPEC.2019.8893531](https://doi.org/10.1109/UPEC.2019.8893531)

Publication date:
2020

Document Version
Peer reviewed version

[Link back to DTU Orbit](#)

Citation (APA):
Rezkalla, M. M. N., & Marinelli, M. (2020). Augmenting System Inertia Through Fast Acting Reserve – A power System Case Study with High Penetration of Wind Power. In *Proceedings of 54th International Universities Power Engineering Conference IEEE*. <https://doi.org/10.1109/UPEC.2019.8893531>

General rights

Copyright and moral rights for the publications made accessible in the public portal are retained by the authors and/or other copyright owners and it is a condition of accessing publications that users recognise and abide by the legal requirements associated with these rights.

- Users may download and print one copy of any publication from the public portal for the purpose of private study or research.
- You may not further distribute the material or use it for any profit-making activity or commercial gain
- You may freely distribute the URL identifying the publication in the public portal

If you believe that this document breaches copyright please contact us providing details, and we will remove access to the work immediately and investigate your claim.

Augmenting System Inertia Through Fast Acting Reserve – A Power System Case Study with High Penetration of Wind Power

Michel Rezkalla, Mattia Marinelli

Center for Electric Power and Energy, Department of Electrical Engineering
Technical University of Denmark (DTU)
Risø Campus, Roskilde, Denmark
Email: matm@elektro.dtu.dk

Abstract—A number of jurisdictions across the world are committed to reducing their carbon emissions. A key route to decarbonisation is by raising the share of renewable generation. However, this will result in reduction of the system inertia and consequently deterioration of frequency stability. Fast acting reserve (FAR) is seen as a possible solution. Various approaches concerning the control of FAR (e.g. frequency gradient and frequency deviation based triggering) have previously been proposed. There is however a lack of clarity regarding the volume of FAR that can potentially compensate for reduction in system inertia. This paper carries out a quantitative assessment of FAR to limit the rate of change of frequency. All island power system of Ireland is adopted as a test case for analysis. The study concludes that FAR can mitigate the RoCoF and it presents also the quantitative relationship between FAR and conventional inertia which depends on system conditions.

Keywords—Fast acting reserves, Frequency stability, Low carbon system, Synthetic inertia.

I. INTRODUCTION

The increasing share of distributed and inertia-less resources entails an increase upsurge in the requirement for balancing and system stabilization services. The reduction of system inertia has mainly two implications with regards to system frequency stability: 1) Faster rate of change of frequency (RoCoF) - resulting in possible tripping of grid components, especially embedded renewable generation, conventional generation pole slipping and cascade tripping. 2) Higher frequency deviations (nadirs/zeniths) potentially leading to unintended load shedding and in worst cases, system collapse. Moreover, the high volatility of renewable energy sources (RES) contributes to the frequency stability issue by changing the grid inertia over time and increasing the need for better planning due to higher uncertainty.

Various transmission system operators (TSOs) with limited AC interconnection have identified these issues to be of critical significance and have initiated mitigation measures. For example, the synchronous power system of the Republic of Ireland and Northern Ireland has an operational constraint of a minimum of 20000 Megawatt-seconds (MWs) of kinetic energy stored in rotating masses of the system, generally addressed as

system inertia floor, which is the sum of each machine's rated power time relative inertia constant H ($E_K = \sum_{i=1}^n H_i S_i$ [MWs]) [1], [2]. Instead of maintaining a minimum inertia floor, such as 20000 MWs, authors in [3] propose an economic dispatch strategy to dynamically calculate the minimum inertia level, leading to reduced inertia requirement in some cases, which still needs to be maintained by conventional plants. The Hydro-Quebec Transenergie's (HQT) transmission connection requirement stipulates in detail that wind power plants must be equipped with an inertia emulation system. HQT is now in the process of procuring and validating manufacturers' models integrating inertia emulation features [4]. Due to the high share of inertia-less resources, National Grid, UK TSO is procuring fast reserves to provide the rapid delivery of power through either increased output from a generator or a reduction in consumption from demand sources, to control frequency changes that might arise from sudden, and sometimes unpredictable, changes in generation or demand [5]–[7].

One can notice that the various solutions previously mentioned and employing inverter connected resources (e.g. energy storage, wind turbine etc.) do not define the quantitative relationship between MW of reserve and the correspondent MWs of synchronous inertia that those will be able to replace. For example, how much MW of fast acting reserve (FAR) will compensate for the reduction of 1 MWs of synchronous inertia?

This work aims at investigating the ability of non-synchronous fast reserves to replace generators' inertia and assessing the quantitative relationship between MW of FAR units (e.g. storage systems) and MWs of synchronous inertia. In this study, the FAR units are represented by a single equivalent unit which represents an aggregated number of units of the same characteristics (e.g. same response time). Two different control mechanisms are investigated, RoCoF based control, addressed further as synthetic inertia control (SIC) and frequency deviation based control, addressed as fast frequency control (FFC) [8], [9]. The analysis is applied on an equivalent model of the Republic of Ireland and Northern Ireland power system.

II. METHODOLOGY

A. Mathematical background

During any disturbance that causes an imbalance between the torques acting on the rotor (i.e. active power imbalance between generation and consumption), the net torque causing acceleration or deceleration is $T_a = T_m - T_e$, where T_m is the mechanical torque applied on the rotor and T_e is the electrical torque on the rotor. The simplest model of electro-mechanical swings in a power system is based on the so called swing equation [10], [11]:

$$T_a = T_m - T_e = J \frac{d\omega_m}{dt} \quad (1)$$

where J is the combined moment of inertia of the generator and the turbine (kgm^2), and ω_m is the angular velocity of the rotor (rad/s).

Formulating the swing equation as in [8], it can be expressed as:

$$\frac{d\bar{\omega}_e}{dt} = \frac{\bar{T}_m - \bar{T}_{e0} - (K_D + K_{FFC})\Delta\bar{\omega}_e}{2H + K_{SIC}} \quad (2)$$

where $\bar{\omega}_e$ is the angular velocity of the electrical rotor, K_D is a damping factor in per unit (pu), K_{FFC} and K_{SIC} are the FFC and SIC proportional control coefficients, respectively and H is the inertia constant.

One can notice that FFC and SIC can affect the RoCoF variation during the transient. Note that due to the response time of FFC and SIC and the power ramp-rate limitations of the used energy source (e.g. battery ramp-rate), it turns out to be a complex time-variant term. However, the presented swing equation shows that mitigating the impact of power imbalances in terms of RoCoF can be achieved by increasing the system rotational inertia H , employing fast reserves with RoCoF based control and/or with frequency deviation based control.

B. System model and generating units

A single busbar equivalent model of the All Island Power System (AIPS), which is the synchronized power system linking the Republic of Ireland and Northern Ireland, has been considered as the study case system [12]. The AIPS is projected for the year 2020, has been developed as a single busbar dynamic model, and has been employed to assess system frequency stability. This model will be described as the single frequency model (SFM). The AIPS is an islanded system with two HVDC connections to Great Britain. An overview of the system installed capacity is represented in Table I. The system has a total dispatchable power of 10064 MW [13].

The SFM is used to examine the frequency behaviour of the power system following the loss of the largest single infeed (LSI). The model had been previously developed on MATLAB/Simulink platform and more details can be found in [12]. The SFM employs a single busbar that concentrates on the energy imbalance of the power system, while ignoring any of the transmission characteristics. The SFM assumes a single busbar and it represents the dynamic interactions of turbines, governors, boilers and load. This model has been developed

TABLE I
THE AIPS INSTALLED CAPACITY AND LOAD

Fuel Type	Installed capacity
Gas and/or distillate oil	6249 MW
Pumped storage hydro	292 MW
Milled peat and biomass	346 MW
Coal and/or heavy fuel oil	1961 MW
Hydro	216 MW
DC interconnector	1000 MW
All wind (partially/non-dispatchable)	5000 MW
Peak load	6900 MW

over many years for the power system of Ireland and Northern Ireland, and it has been validated based on the manufacturers' data and real event traces to provide accurate traces of the overall system frequency response in the first 30 s following significant generation/demand imbalance events [14], [15].

The SFM model includes all of the generators present in the AIPS fed by any desired dispatch. Fixed speed wind turbines and variable speed wind turbines are modelled separately to recognize the inertia contribution from the fixed speed turbines. A schematic layout of the single bus frequency model is shown Fig. 1. The Plexos production cost modelling tool was used to simulate hourly dispatch schedules for the year 2020. In this study, 780 dispatches that are representative of different operational scenarios, are used.

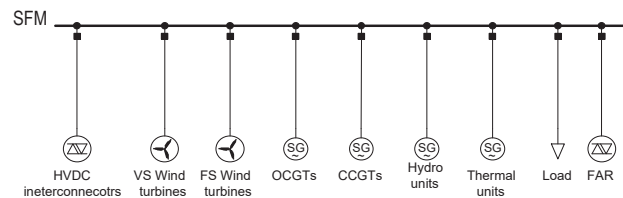


Fig. 1. The single frequency model representation

C. Methodology

This study applies a bottom-up inductive approach for a quantitative evaluation of synchronous inertia, which can be potentially replaced by a specified magnitude of FAR. The inductive approach provides a systematic set of procedures for analyzing data that can produce reliable and valid findings. This study employs two different control mechanisms for FAR, namely SIC and FFC. The method begins by examining the RoCoF following the loss of the LSI and it then removes one conventional plant and its associated inertia, which is substituted with FAR. An equivalence is established when the RoCoF value from the pre-plant removal and post FAR addition equalizes. This process will be done over a large number of dispatches. It has been decided to calculate the RoCoF over a 500 ms moving window, similar to the RoCoF

relay's requirements in the Irish grid code [1]. A flow chart of the applied method is presented in Fig. 2 and the following procedure is used:

- 1) Apply a simulated system dispatch (e.g. dispatch A) to the SFM, and then evaluate the system frequency and RoCoF following the loss of the LSI.
- 2) Dispatch A is modified by removing a conventional plant and its associated inertia, and then re-dispatching the power of the removed plant over the remaining ones (dispatch A'). The LSI must remain the same as in dispatch A.
- 3) Add FAR reserves to the modified dispatch to compensate for the removed inertia. An equivalence between the MW of FAR and the MWs of synchronous inertia is established when the maximum average RoCoF from the pre-plant removal and post FAR addition equalizes.

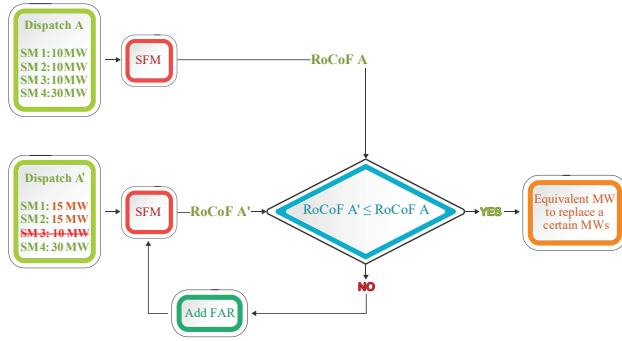


Fig. 2. Applied methodology flow chart

The implemented control diagrams of the SIC and FFC are represented in Fig. 3-a and Fig. 3-b, respectively. The proportional control (K_{SIC} and K_{FFC}) are calculated through an iteration process to determine the required amount of reserves that are able to compensate for the reduced synchronous inertia, as previously explained in the methodology.

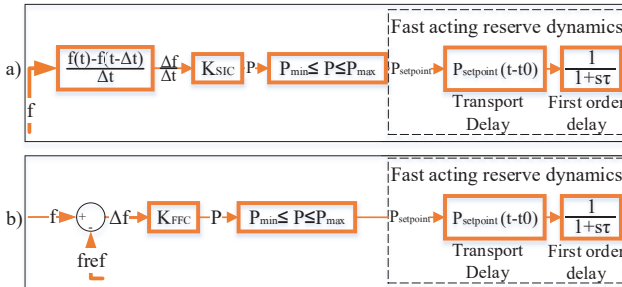


Fig. 3. SIC and FFC control diagram

III. RESULTS AND DISCUSSION

Four different scenarios are analyzed. In all four scenarios, the system response is triggered by the loss of the LSI, which varies over the different dispatches. A brief description of different scenarios follows:

- Scenario 1: The first scenario investigates the ability of SIC and FFC in mitigating the RoCoF and their effects on the system stability. Applying the proposed methodology, this scenario presents the performance of the two control mechanisms when two different dispatches are applied: high inertia and low inertia dispatches.
- Scenario 2: This scenario uses 780 dispatches and applies the proposed methodology. The second scenario determines the relationship between MW of FAR and MWs of equivalent synchronous inertia.
- Scenario 3: The third scenario carries out a sensitivity analysis of the FAR's response time. It highlights the response time's effects on the system stability, and on the relationship between MW and MWs. Response times of 50 ms, 100 ms and 150 ms are used.
- Scenario 4: This scenario carries out a sensitivity analysis of the deadband applied on the control signal. The following values are used for FFC: 80 mHz, 120 mHz and 300 mHz. Similarly, for the SIC the following values are used: 80 mHz/s, 120 mHz/s and 300 mHz/s.

A. Scenario 1

The first scenario analyzes the capability of FFC and SIC to limit the RoCoF and their effects on the system stability. The following deadbands are used: 80 mHz and 80 mHz/s for FFC and SIC, respectively, and 50 ms response time is applied. Using the system inertia as a metric, two different dispatches are investigated: high inertia case and low inertia case, respectively, 36855 MWs and 16649 MWs. It should be noted that the SFM does not consider the loads' inertia contribution, therefore, the system inertia is composed only by the generations' inertia. The system frequency, RoCoF and energy storage's active power for the high inertia case are presented in Fig. 4.

As previously demonstrated in (2), Fig. 4 shows the ability of the two controllers in mitigating the RoCoF. Because of the different control approaches (i.e. FFC and SIC) and the applied deadbands, different amounts of MW were needed to replace the same amount of MWs of synchronous inertia. This point will be further addressed in Scenarios 2 and 3 by employing more dispatches. It can be noted that the FFC required roughly the double amount of MW compared to SIC, which is due to the different deadbands.

Although this study does not aim to improve the system frequency (i.e. in terms of nadir and steady state value), the FFC has a better performance compared to the SIC. In other words, the employment of FFC to mitigate the RoCoF will implicitly support the system frequency, improving the overall system stability.

In the case of low inertia (i.e. 16649 MWs), Fig. 5 shows the ability of FFC and SIC to mitigate the maximum average RoCoF value by compensating for the reduced generation's inertia. Because of the system's low inertia, the frequency deviation was larger and steeper. This led to faster activation of the FFC compared to the high inertia case. However, the FFC still requires a larger amount of MW to compensate for the reduced

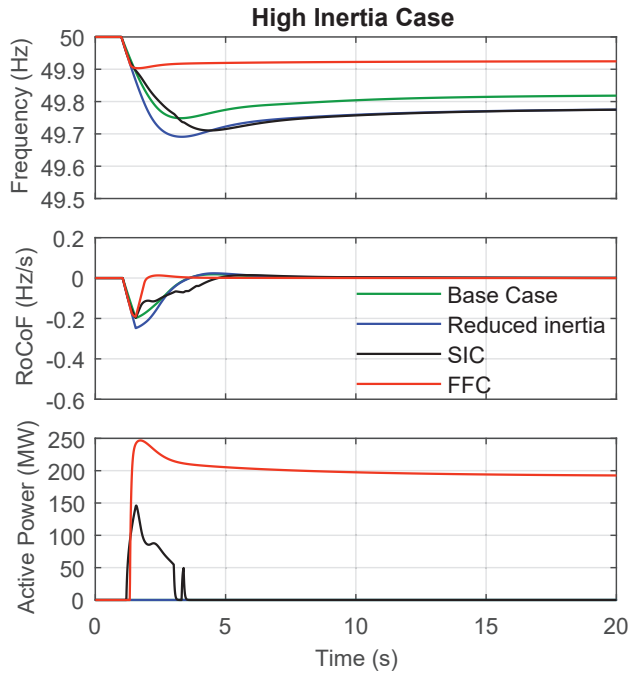


Fig. 4. System frequency and RoCoF - High inertia

generators' inertia compared to the SIC. In this case, the SIC was triggered before FFC due to the different deadband.

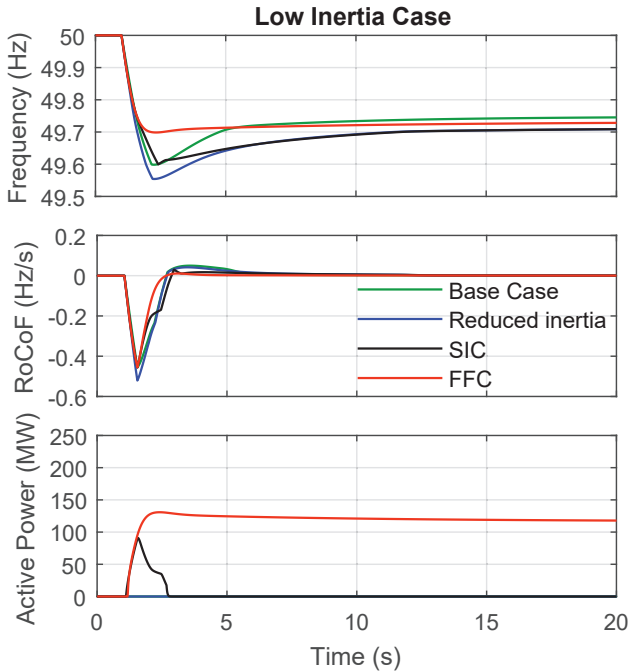


Fig. 5. System frequency and RoCoF - Low inertia

B. Scenario 2

In the second scenario, 780 dispatches are used. This scenario aims to define the relationship between 1 MW of FFC (or SIC) and MWs of synchronous inertia. Applying the previously proposed methodology over the various dispatches, Fig. 6 shows the relationship between MW to MWs and maximum average RoCoF (i.e. measured over 500 ms) for the FFC control approach. The Y axis represents the MWs that can be replaced by 1 MW of FFC while the X axis represents the maximum average RoCoF following the loss of the LSI. The blue dots represent the different dispatches. Although the relationship between MW to MWs is not constant over the different dispatches, one can see a clear trend between the MW to MWs and the system maximum average RoCoF. Using MATLAB's fitting algorithm, it was possible to determine the 3rd order polynomial regression among the different dispatches, which is represented by the following function: $y = -3.3e03x^3 - 3.8e03x^2 - 1.4e03x - 1.2e02$.

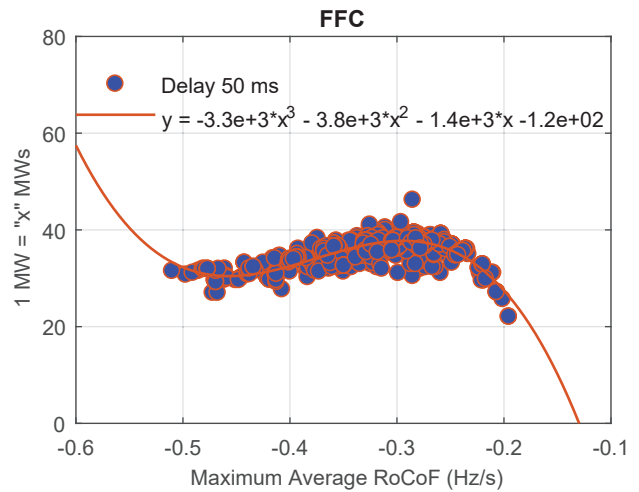


Fig. 6. Relationship between MW/MWs and RoCoF - FFC

For low inertia cases and/or larger infeed loss (i.e. fast RoCoF), the equivalent MWs of inertia that can be substituted with 1 MW of FFC is decreasing. Meanwhile, due to the applied deadband as shown and explained in Scenario 1, for high inertia cases and/or small infeed loss, the equivalent MWs of inertia to 1 MW of FFC is also decreasing.

The same study is performed with the SIC controller. Fig. 7 shows the relationship between MWs to MW and the system maximum RoCoF for the SIC control approach. The same dispatches are used.

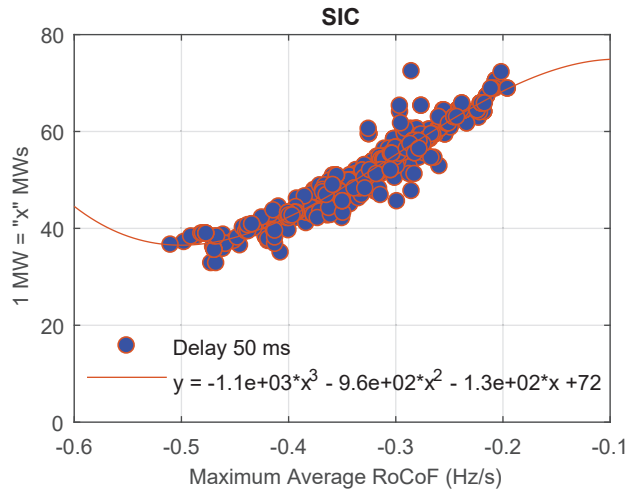


Fig. 7. Relationship between MW/MWs and RoCoF - SIC

As in the FFC, for low inertia cases and/or larger infeed loss (i.e. fast RoCoF), the equivalent MWs of inertia that can be substituted with 1 MW of SIC are lower than for high inertia cases. In contrast, for high inertia cases, the equivalent MWs of inertia to 1 MW of SIC are not decreasing, as for FFC. This behaviour is mainly due to the different deadband between the two controllers. In other words, the 80 mHz/s deadband does not limit the SIC participation, as the 80 mHz does for FFC.

C. Scenario 3

A sensitivity analysis of the device's response time is carried out to better understand the effects of the fast acting reserves' time response on the relationship between MW and MWs, and on the overall system stability. The following time delays (i.e. response time) are applied: 50 ms, 100 ms and 150 ms. The chosen values are inspired from different energy storage manufacturers' data-sheets [16]–[18].

Fig. 8 shows the time delay effect on the relationship between MW and MWs when FFC is applied. It can be noted that the larger response time reduced the FFC effects on mitigating the RoCoF, leading to the need of larger reserves. However, in some dispatches, the larger response time led to frequency oscillations and, therefore, no solution was found. Due to the delay, the controller is acting on system conditions that were occurring, for example, 150 ms in the past and not on the current conditions. For dispatches with high inertia and/or small infeed loss, employing 150 ms delay with the 80 mHz deadband, the controller was unable to mitigate the maximum average RoCoF because it was occurring before the unit's response (i.e. which is represented by zero on the x axes). Fig. 8 points out that the units' characteristics (e.g. response time, ramp rate etc.) will influence the 3rd order regression and, therefore, the method needs to be applied for each group of units of certain characteristics that are allowed to participate in this grid service.

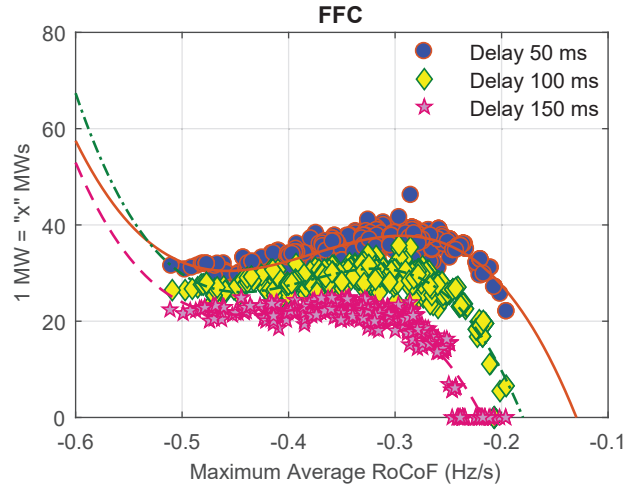


Fig. 8. Response time sensitivity analysis - FFC

D. Scenario 4

To better investigate the effects of the used deadband on the controllers' performance and on the relation between MW and MWs, this scenario carries out a sensitivity analysis on the deadband applied on the control signal. Since this study assumes that this inertia service is a contingency based service, it has been decided to use deadband values relatively larger than the frequency deadband present on conventional generators and interconnectors established by the grid code [19]. In this study, the following deadband values are used for FFC: 80 mHz, 120 mHz and 300 mHz. Similarly, for the SIC the following deadband values are used: 80 mHz/s, 120 mHz/s and 300 mHz/s.

Fig. 9 shows that the larger deadband reduced the effects of FFC in mitigating the RoCoF. Employing 120 mHz deadband, for high inertia cases and/or small infeed loss, the controller was unable to influence the maximum average RoCoF because it was occurring within the applied deadband. Applying 300 mHz deadband, FFC was unable to participate in any of the dispatches because all of the congestions were occurring within the deadband. On the one hand, employing a large deadband will limit the FFC participation to large congestion cases avoiding its activation following normal load change. On the other hand, Fig. 9 points out that employing a large deadband will reduce the equivalent MWs that can be replaced by 1 MW of FFC as might also make the controller completely useless as the case with 300 mHz deadband.

Fig. 10 shows that the larger deadband reduces the equivalent MWs that can be replaced by 1 MW of SIC. For low inertia cases and/or larger infeed loss (i.e. fast RoCoF), one can notice that when applying 120 mHz/s deadband the SIC performance did not differentiate so much from 80 mHz/s deadband. Employing 300 mHz/s deadband limited the SIC participation for the majority of dispatches and imposed oscillation for the remaining ones.

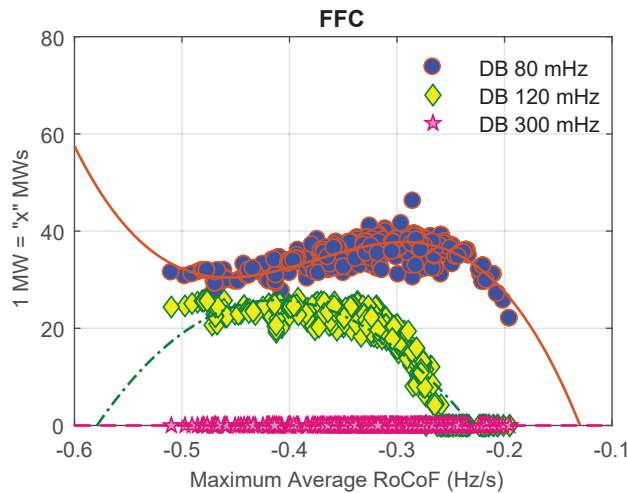


Fig. 9. Deadband sensitivity analysis - FFC

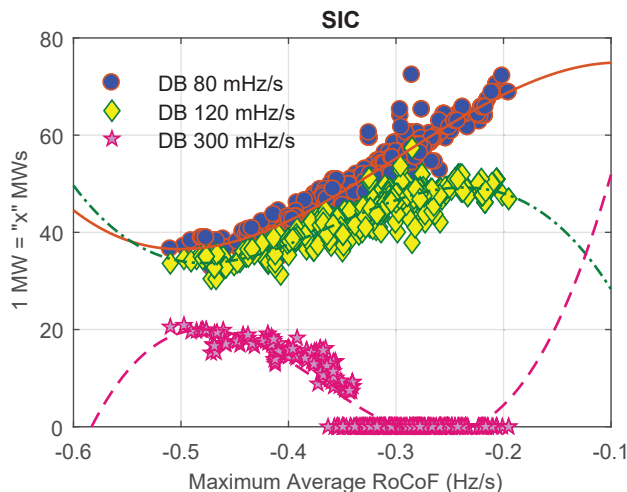


Fig. 10. Deadband time sensitivity analysis - SIC

IV. CONCLUSION AND FUTURE WORKS

This work has shown the ability of FAR to mitigate the RoCoF when these reserves are controlled by frequency deviation based control or by RoCoF based control. By exploiting 780 simulated dispatches of the AIPS, validated against real measurement data, it was possible to define an analytical relationship between MW of reserve and MWs of synchronous inertia for the two applied control mechanisms (i.e. FFC and SIC). Future work will consider the activation of the reserves based on a threshold to analyze the effects and possibility of mitigating the RoCoF through a threshold based control using both FFC and SIC. Further analysis will also analyze the effects of measuring the RoCoF over a different time window on the controllers' performance and the frequency stability. Also, various control technique such as hysteresis control will be investigated to understand and counteract the

frequency oscillation due to the implementation of the two controllers.

ACKNOWLEDGMENT

The authors would like to thank EirGrid, the TSO of the Republic of Ireland, for providing the equivalent model of the all island power system as well as the needed data.

REFERENCES

- [1] DNV GL Energy Advisory, "RoCoF Alternative Solutions Technology Assessment," tech. rep., EIRGRID, 2015.
- [2] EirGrid-Group, "Operational Constraints Update," Tech. Rep. October, EirGrid-Group, 2015.
- [3] P. Daly, D. Flynn, and N. Cunniffe, "Inertia Considerations within Unit Commitment and Economic Dispatch for Systems with High Non-Synchronous Penetrations," in *PowerTech IEEE*, (Eindhoven), pp. 1–6, 2015.
- [4] J. Brisebois and N. Aubut, "Wind Farm Inertia Emulation to Fulfill Hydro-Québec's Specific Need," in *Power and Energy Society General Meeting IEEE*, vol. 7, pp. 1–7, 2011.
- [5] National Grid, "Fast Reserve Service Description," Tech. Rep. April, NationalGrid, 2013.
- [6] A. Junyent-Ferré, Y. Pipelzadeh, and T. C. Green, "Blending HVDC-Link Energy Storage and Offshore Wind Turbine Inertia for Fast Frequency Response," *IEEE Transactions on Sustainable Energy*, vol. 6, no. 3, pp. 1059 – 1066, 2015.
- [7] B. Silva, C. L. Moreira, L. Seca, Y. Phulpin, and J. A. P. Lopes, "Provision of Inertial and Primary Frequency Control Services Using Offshore Multiterminal HVDC Networks," *IEEE TRANSACTIONS ON SUSTAINABLE ENERGY*, vol. 3, no. 4, pp. 800–808, 2012.
- [8] M. Rezkalla, A. Zecchino, S. Martinenas, A. M. Prostejovsky, and M. Marinelli, "Comparison between Synthetic Inertia and Fast Frequency Containment Control Based on Single Phase EVs in a Microgrid," *Applied Energy*, pp. 1–12, 2017.
- [9] M. Rezkalla, M. Marinelli, M. Pertl, and K. Heussen, "Trade-off Analysis of Virtual Inertia and Fast Primary Frequency Control during Frequency Transients in a Converter Dominated Network," in *Innovative Smart Grid Technologies - Asia (ISGT-Asia)*, IEEE, (Melbourne, VIC, Australia), pp. 1–6, 2016.
- [10] P. Kundur, J. Paserba, V. Ajarapu, G. Andersson, A. Bose, C. Canizares, N. Hatziargyriou, D. Hill, A. Stankovic, C. Taylor, T. Van Cutsem, and V. Vittal, "Definition and Classification of Power System Stability," *IEEE Transactions on Power Systems*, vol. 21, no. 3, pp. 1387–1401, 2004.
- [11] A. Prostejovsky, M. Marinelli, M. Rezkalla, M. Syed, and E. Guillo-Sansano, "Tuningless Load Frequency Control Through Active Engagement of Distributed Resources," *IEEE Transactions on Power Systems*, vol. 33, no. 3, pp. 2929 – 2939, 2017.
- [12] J. O'Sullivan and M. O'Malley, "Identification and Validation of Dynamic Global Load Model Parameters for Use in Power System Frequency Simulations," *IEEE Transactions on Power Systems*, vol. 11, no. 2, pp. 851–857, 1996.
- [13] EirGrid and SONI, "All-Island Generation Capacity Statement," tech. rep., EirGrid, 2017.
- [14] J. O'Sullivan, A. Rogers, and A. Kennedy, "Determining and implementing an approach to system frequency and inertial response in the Ireland and Northern Ireland power system," in *Power and Energy Society General Meeting IEEE*, pp. 1–6, 2011.
- [15] J. O'Sullivan, A. Rogers, D. Flynn, S. Member, P. Smith, A. Mullane, and M. O'Malley, "Studying the Maximum Instantaneous Non-Synchronous Generation in an Island System — Frequency Stability Challenges in Ireland," *IEEE Transactions on Power Systems*, vol. 29, no. 6, pp. 2943–2951, 2014.
- [16] International Electrotechnical Commission, "Electrical Energy Storage," tech. rep., International Electrotechnical Commission, 2011.
- [17] US Department of Energy, "Grid Energy Storage," no. December, pp. 1–67, 2013.
- [18] M. Rezkalla, M. Pertl, and M. Marinelli, "Electric Power System Inertia : Requirements , Challenges and Solutions," *Springer Electrical Engineering*, vol. 100, no. 4, pp. 2677–269, 2018.
- [19] N. W. Miller, M. Shao, S. Pajic, and R. D. Aquila, "NREL," Tech. Rep. May, NGK INSULATORS, 2013.